

Phys. Rev. Lett. **39**, 1529 (1977).

<sup>2</sup>D. W. Forslund, J. M. Kindel, and K. Lee, Phys. Rev. Lett. **39**, 284 (1977).

<sup>3</sup>Kent Estabrook and W. L. Kruer, Phys. Rev. Lett. **40**, 42 (1978).

<sup>4</sup>C. E. Max and K. G. Estabrook, Comments Plasma Phys. Controlled Fusion **5**, 239 (1980).

<sup>5</sup>A. G. M. Maaswinkel, K. Eidmann, and R. Sigel, Phys. Rev. Lett. **42**, 1625 (1979).

<sup>6</sup>E. Fabre, in Proceedings of the International Atomic Energy Agency Technical Committee Meeting on Advances in Inertial Confinement Systems, Osaka, 1980 (unpublished), p. 28.

<sup>7</sup>V. C. Rupert, E. M. Campbell, D. W. Phillion, and F. Ze, in Proceedings of the Tenth Annual Anomalous Absorption Conference, San Francisco, May 1980 (unpublished).

<sup>8</sup>Stephen B. Segall, J. Appl. Phys. **51**, 206 (1980).

<sup>9</sup>C. E. Thomas, Appl. Opt. **14**, 1267 (1975).

<sup>10</sup>K. R. Manes *et al.*, J. Opt. Soc. Am. **67**, 717 (1977).

<sup>11</sup>K. A. Brueckner, Phys. Rev. Lett. **36**, 677 (1976).  
Note that the right-hand side of Eq. (3) is too large by a factor of 2.

<sup>12</sup>H. Brysk, Phys. Rev. Lett. **37**, 1242 (1976).

<sup>13</sup>J. A. Tarvin and R. J. Schroeder, KMS Fusion Report No. U-1033 (to be published).

<sup>14</sup>R. S. Craxton and R. L. McCrory, University of Rochester, Laboratory for Laser Energetics Report No. 108 (unpublished).

<sup>15</sup>D. J. Tanner, D. Mitrovich, R. L. Berger, J. A. Tarvin, and J. Larsen, Bull. Am. Phys. Soc. **25**, 895 (1980), and in Proceedings of the Tenth Annual Anomalous Absorption Conference, San Francisco, May 1980 (unpublished).

## Experimental Studies of the Bilateral Ion Blowoff from Laser-Irradiated Thin Plastic Foils

G. D. Tsakiris,<sup>(a)</sup> K. Eidmann, R. Petsch, and R. Sigel

*Projektgruppe für Laserforschung, Max-Planck-Gesellschaft zur Förderung der Wissenschaften e.V.,*

*D-8046 Garching, Federal Republic of Germany*

(Received 25 September 1980)

Thin plastic foils of various thicknesses (0.13–5.0  $\mu\text{m}$ ) were irradiated by iodine-laser pulses with an incident intensity of  $4 \times 10^{15} \text{ W cm}^{-2}$ . Time-of-flight charge collectors and a Thomson parabola mass spectrometer were used to measure the asymptotic ion velocity distribution at the back and the front (laser) sides of the target. Analysis of these data yielded the ratios of the hot-electron densities and of the hot-electron temperatures at both sides of the foil target. The results disagree with calculations based on classical electron penetration into the foil.

PACS numbers: 52.50.Jm, 52.70.Nc

A major complication of the laser-target interaction problem in laser fusion derives from the fact that a significant fraction of the absorbed laser energy is coupled into a hot-electron component. These hot electrons affect the target behavior in at least two important ways: (i) they create a large electrostatic field in the corona, thus causing fast-ion acceleration and (ii) because of their long range, they may deeply penetrate and preheat the target. These effects may strongly modify the hydrodynamic response of laser-irradiated implosion targets; thin-walled shell targets, for example, have been found to obey a so-called exploding, rather than ablative-ly driven, pusher mode for the energy deposition by fast electrons. Though the subject has been studied for some time in the history of laser fusion,<sup>1</sup> it is still far from quantitative resolution.

For studying the penetration of fast electrons into and through the wall of the target implosion experiments have a certain disadvantage because of their necessarily "closed" spherical geometry.

Experiments in planar geometry using thin-film targets avoid this difficulty since the rear (inner) side becomes accessible. In particular, it then becomes possible to study energy transport through a target by comparing ion emission from both surfaces. Indeed, previous workers have exploited this concept to some extent in studies of reduced thermal conductivity<sup>2</sup> and, more recently, wavelength dependence of laser-target interaction.<sup>3</sup> In this paper we present for the first time detailed ion spectra from the front and rear sides as a function of target thickness. These data allow *quantitative* comparison with continuing theoretical studies of fast electron transport. We shall show on the basis of simple models that the results greatly differ from expectations based on classical electron penetration into the foil. We note that in scope—though not in method—our investigation is similar to recent spectroscopic studies of fast-electron-excited  $K\alpha$  radiation from layered targets.<sup>4</sup>

The experiments were carried out with 65-J

(average), 300-ps [full width at half maximum (FWHM)] pulses from the Asterix III iodine laser ( $\lambda = 1.3 \mu\text{m}$ ). Focused with an aspherical  $f/2$  lens, the focal spot diameter (for half-energy) was  $60 \mu\text{m}$ , corresponding to an incident light intensity of  $4 \times 10^{15} \text{ W cm}^{-2}$ . Thin films were stretched on a plane steel holder with holes 3 mm in diameter. The film material was low- $Z$  plastic, either  $\text{C}_6\text{H}_7\text{O}_{11}\text{N}_3$  with  $A = 11, Z = 5.6$  for a foil thickness  $d_F < 1 \mu\text{m}$  or  $\text{C}_{16}\text{O}_3\text{H}_{14}$  with  $A = 7.7, Z = 5.0$  for  $d_F > 1 \mu\text{m}$ . The ion diagnostics consisted of a Thomson parabola mass spectrometer with cellulose nitrate film ( $7\text{-}\mu\text{m}$  thick sensitive layer) as detector and charge collectors ( $A\text{-}F$ ) at distances of typically 170 cm from the target. The geometrical arrangement is shown in the inset of Fig. 1. The collectors  $A$  and  $B$  were located in the direction of the target normal (at  $30^\circ$  to the laser axis) in the front and rear spaces, respectively; they were used to study the symmetry of ion emission as shown later in Fig. 2. Collectors  $C\text{-}F$  allowed the angular distribution of the ion emission to be measured. The pressure in the chamber (including TP housing) was kept below a few times  $10^{-6}$  Torr to avoid charge exchange. Details on the construction and testing of the collectors and the Thomson parabola will be published elsewhere.

Figure 1 compares time-of-flight (TF) and Thomson parabola (TP) data from the same shot. Note that these data have *not* been normalized to

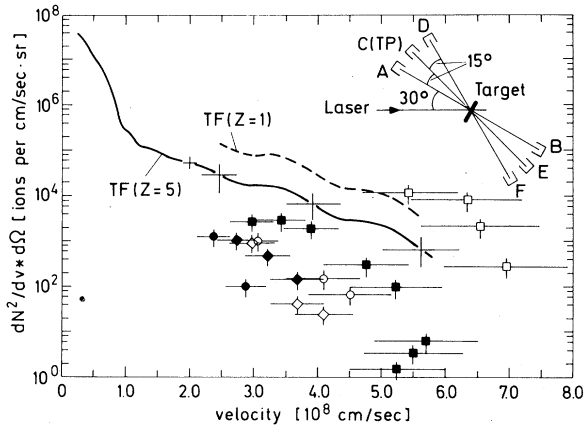


FIG. 1. Comparison of the time-of-flight (TF) and Thomson parabola (TP) data. The points are from the TP and represent different ion species: solid squares:  $\text{O}^{+8}, \text{N}^{+7}, \text{C}^{+6}$ ; circles:  $\text{O}^{+7}$ ; solid circles:  $\text{O}^{+6}$ ; diamonds:  $\text{N}^{+6}$ ; solid diamonds:  $\text{N}^{+5}$ ; squares:  $\text{H}^{+1}$ . The inset shows the geometrical arrangement of the detectors. TF collectors  $C$  or  $E$  were in some shots replaced by the TP.

each other. The TP data show preferential proton acceleration as has been observed previously.<sup>5</sup> Otherwise, the fully stripped ion species with  $A/Z = 2$  ( $\text{O}^{+8}, \text{N}^{+7}, \text{C}^{+6}$ ) are dominant, i.e., the plasma is found to be fully ionized. In order to compare the TF with the TP data, an assumption about the average  $Z$  of the plasma is required. An average  $Z = 5$  (solid line) seems to be more appropriate for the bulk of the plasma, and  $Z = 1$  (dashed line) for the front. This uncertainty with respect to  $Z$  affects the energy and mass determination of the fast ions within a factor  $(A/Z):(A_H/Z_H) = 1.5\text{-}2.0$ , and their total number within a factor  $Z/Z_H = 5$ . Here and in the following we consider—somewhat arbitrarily—fast ions as those with a velocity higher than  $1.6 \times 10^8 \text{ cm s}^{-1}$ , i.e., beyond the dip in the ion spectra.

The energy angular distribution [ $dE(\Theta)/d\Omega$ ] for the fast-ion component measured with the charge collector array shows a very directional pattern around the target normal. The FWHM of the frontal distribution appears to be independent of the foil thickness and about  $18^\circ$ . In contrast, the rear distribution has a FWHM of  $18^\circ$  for  $d_F \leq 0.3 \mu\text{m}$ , while for  $d_F > 1.0 \mu\text{m}$  the FWHM is  $36^\circ$ . These data are used to obtain the fractional energy loss of fast ions  $(E_{h,B} + E_{h,F})/E_{\text{abs}}$ . In the limit of thick foils ( $d_F \geq 1 \mu\text{m}$ ) the main fast-ion loss occurs on the front side and amounts to a fraction of 0.2–0.3. This value is much higher than the fraction  $\approx (zm_e/m_i)^{1/2}$  expected by relating fast-ion losses due to an outward, hot-electron-driven rarefaction wave to free inward streaming of the hot electrons.<sup>6</sup> Such enhanced losses have been observed in many experiments<sup>1</sup> and have been interpreted as an indication of reduced inward transport.<sup>7</sup> Note that the observation of enhanced fast-ion losses in our experiment is qualitatively consistent with the discrepancy found relative to classical penetration of the electrons into the foil (see discussion below).

Figure 2 shows ion spectra (averaged over ten shots under identical conditions) measured with the collectors  $A$  and  $B$  in the front and rear space of the target. Parameter is the foil thickness. The spectra have the well-known, characteristic shape which may be connected with a two-temperature, isothermal rarefaction wave.<sup>8,9</sup> As far as the cold temperature  $T_c$  is concerned ( $T_{c,F} \approx 1 \text{ keV}$  independently of foil thickness;  $T_{c,B}$  decreases with foil thickness), it is unclear to what extent it is influenced by recombination in the expanding, dense foil material;  $T_c$  is therefore not discussed further.

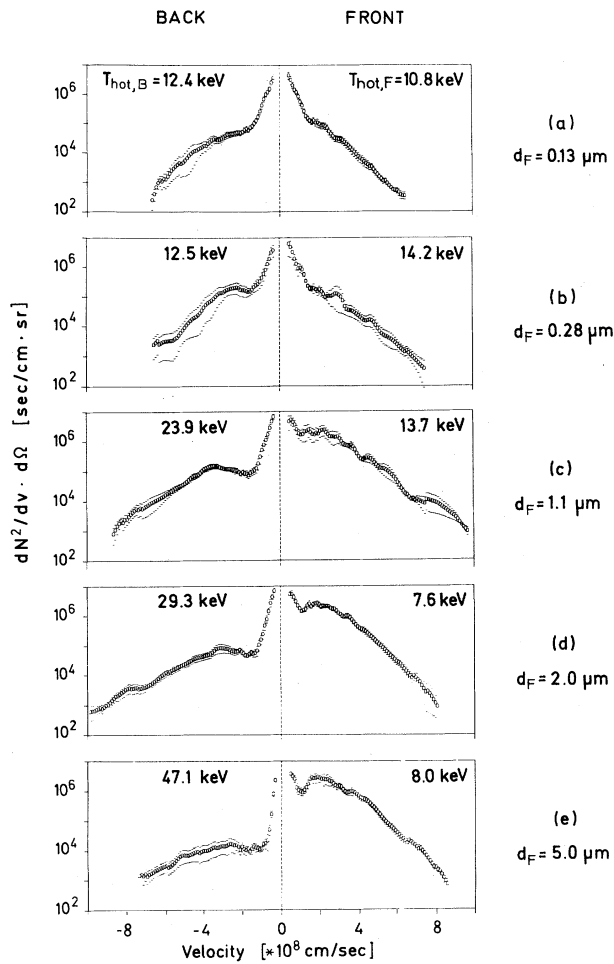


FIG. 2. Bilateral ion velocity spectra for the five foil thicknesses indicated. Front side is laser side.

The main interest here is in the characteristics of fast-ion blowoff, which should not be affected by recombination. The hot temperature  $T_h$  as determined from the high-energy part of the spectrum is given in Fig. 2. We note the following observations: (i)  $T_{h,F}$  shows no systematic variation with foil thickness. Its mean value is  $T_{h,F} \approx 11$  keV, comparable with x-ray hot-electron temperatures ( $\approx 20$  keV) found in this experiment and also with theoretical scaling laws<sup>10</sup>; the latter yield  $T_h \approx 15$  keV for a cold temperature of 0.5–1 keV. (ii)  $T_{h,B}$  systematically increases with foil thickness up to nearly 50 keV. This observation is interpreted as a filtering effect of the foil as expected under conditions where the range of the electrons increases with energy. Indeed we have seen this effect in our classical calculations of electron penetration (see below).

However, it is probably not very specific to classical electron penetration and may be expected from alternative transport models as well. (iii) The ion spectra are symmetric (with respect to the front and rear spaces) only for the thinnest foils ( $d_F \leq 0.3 \mu\text{m}$ ); with increasing foil thickness the number of fast ions observed at the rear gradually diminishes. With 10- $\mu\text{m}$  foils fast ions at the rear could no longer be detected.

We now analyze the experimental observations using a simple model which allows us to relate the ion data to fast-electron transport through the foil. We assume a planar geometry; this means, in particular, that the fast ions are generated on equal areas on the front and rear surfaces. We model the fast-ion expansion on the front and rear sides of the foil by plane rarefaction waves with temperatures  $T_{h,F}$  and  $T_{h,B}$ , respectively. Then, with the energy  $E$  in the rarefaction wave being proportional to  $E \propto n_h s_h^3$  ( $n_h$  is the initial electron density at the point where the wave originates;  $s_h$  is the sound velocity), we can write

$$\frac{n_{h,B}}{n_{h,F}} = \left( \frac{T_{h,F}}{T_{h,B}} \right)^{3/2} \left( \frac{E_B}{E_F} \right)_{\text{fast ions}}$$

The ratio of the hot-electron densities at the back and front surfaces is thus expressed in terms of experimentally measured quantities. Two-temperature effects, such as the formation of rarefaction shocks for  $T_h/T_c > 10^8$  have little effect on this result. The experimentally obtained back-to-front hot-electron density ratios are shown in Fig. 3.

For comparison we have calculated  $n_{h,B}/n_{h,F}$  on the assumption that the hot electrons penetrate into the target according to their classical range. These calculations predict the distribution function of hot electrons at a certain depth in a semi-infinite target for a given frontal distribution function. They are based on tabulated results for the passage of monoenergetic electrons through matter.<sup>11</sup> Calculated curves  $n_{h,B}/n_{h,F}$  are shown in Fig. 3 for an *isotropic* Maxwellian electron source with temperatures of this experiment. We note that our model neglects reflection of electrons at the rear plasma boundary and may therefore underestimate  $n_{h,B}$ . In fact, more sophisticated computer simulations<sup>12, 13</sup> of the electron diffusion into the foil give higher values for  $n_{h,B}/n_{h,F}$  (see Fig. 3). These calculations also include resistive electric fields and (Ref. 13) self-generated magnetic fields.

Comparison of the experimental and calculated

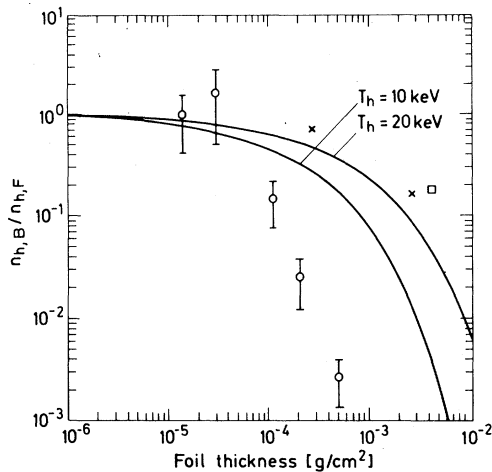


FIG. 3. The ratio of hot-electron densities at the back and front sides of the foil target. The points (circles) represent the measured values. The theoretical curves (solid lines) are based on the classical range of the hot electrons. For comparison we show also results from computer simulations: crosses: glass-foil,  $T_h = 15$  keV, one-dimensional simulation, Ref. 12; square:  $\text{CH}_2$  foil,  $T_h = 20$  keV, two-dimensional simulation, Ref. 13.

values in Fig. 3 shows a large discrepancy; for a  $5\text{-}\mu\text{m}$  ( $\approx 5 \times 10^{-4}$  g/cm<sup>2</sup>) foil target the hot-electron density at the rear of the target is nearly 100 times lower than predicted. Obviously, the model does not describe the experimental observations. This result is remarkable insofar as the assumption of classical penetration of the electrons into the target is common in computer modeling of laser fusion experiments.

At this point it must be mentioned, however, that there is also some disagreement among experiments. Results from thin-film irradiation experiments<sup>3</sup> seem consistent with ours; from spectroscopic studies on layered targets<sup>4</sup> classical penetration of the hot electrons into the target is inferred. The cause for this discrepancy is not yet understood.

The emphasis in this paper is on the presentation of a new set of experimental data rather than on their final interpretation. In particular, one cannot conclude on the basis of the available information that the observations must have to do with anomalous transport inhibition of the fast electrons. If we follow recent computational work<sup>14</sup> (see also the references therein on other theoretical work), it is not even clear from a theoretical point of view whether ion-acoustic turbulence or resistive electric fields—mechan-

isms often quoted in this context—significantly modify energy deposition.

The knowledge gap hitherto preventing any final interpretation concerns the unknown trajectories of the fast electrons. Recent experiments with the  $\text{CO}_2$  laser<sup>15</sup> suggest that the fast electrons may transport a significant fraction of the absorbed energy over distances of several millimeters *along the target surface*. In such a situation the electron distribution function would obviously be highly anisotropic in contrast to our assumption. Furthermore, the electrons may spread out to distances larger than the 3 mm diameter of the hole in the target holder, thus invalidating the assumption of equal areas of fast-ion generation on the front and rear surfaces of the foil. On the basis of the available information such effects cannot be excluded in our experiment.

It may be interesting to note in this context that two-dimensional hydrodynamic effects that occur during foil irradiation and acceleration are most probably not the cause of the observed discrepancies. Two-dimensional flow will, in general, lead to lateral loss of material initially situated under the irradiated surface. This will decrease the integral  $\int_{\text{front}}^{\text{rear}} n_i dl$  ( $n_i$  is the ion density in the target), which, for binary collisions, determines the range of the fast electrons. Such effects should therefore increase rather than decrease the fast-electron transmission through the foil.

There is considerable interest in planar-target experiments as technically less complicated model experiments for laser fusion. Should long-range transport along the surface indeed *dominate* in these experiments, their relevance to spherical laser fusion targets with finite surface area would no longer be obvious. It is clear that the subject urgently calls for further investigation.

<sup>(a)</sup>Present address: Department of Physics and Astronomy, University of Maryland, College Park, Md. 20742.

<sup>1</sup>*Laser-Plasma Interactions*, edited by R. A. Cairns and J. J. Sanderson (SUSSP Publications, Edinburgh, 1980).

<sup>2</sup>J. S. Pearlman and J. P. Anthes, *Appl. Phys. Lett.* **27**, 581 (1975).

<sup>3</sup>F. Amiranoff, R. Fabbro, E. Fabre, C. Garban, J. Virmont, and M. Weinfeld, *Phys. Rev. Lett.* **43**, 522 (1979).

<sup>4</sup>J. D. Hares, J. D. Kilkenny, M. H. Key, and J. G. Lunney, *Phys. Rev. Lett.* **42**, 1216 (1979).

- <sup>5</sup>R. Decoste and B. H. Ripin, *Phys. Rev. Lett.* **40**, 34 (1978).
- <sup>6</sup>R. L. Morse and C. W. Nielson, *Phys. Fluids* **16**, 909 (1973).
- <sup>7</sup>P. M. Campbell, R. R. Johnson, F. J. Mayer, L. V. Powers, and D. C. Slater, *Phys. Rev. Lett.* **39**, 274 (1977).
- <sup>8</sup>B. Bezzerides, D. W. Forslund, and E. L. Lindman, *Phys. Fluids* **21**, 2179 (1978).
- <sup>9</sup>L. M. Wickens, J. E. Allen, and P. T. Rumsby, *Phys. Rev. Lett.* **41**, 243 (1978).
- <sup>10</sup>D. W. Forslund, J. M. Kindel, and K. Lee, *Phys. Rev. Lett.* **39**, 284 (1977); K. Estabrook and W. L. Kruer, *Phys. Rev. Lett.* **40**, 42 (1978).
- <sup>11</sup>L. V. Spencer, *Energy Dissipation by Fast Electrons*, National Bureau of Standards Monograph No. 1 (U. S. GPO, Washington, D. C., 1959).
- <sup>12</sup>D. Shvarts, C. Yablon, I. B. Bernstein, J. Virmont, and P. Mora, *Nucl. Fusion* **19**, 1457 (1979).
- <sup>13</sup>R. J. Mason, *Phys. Rev. Lett.* **42**, 239 (1979).
- <sup>14</sup>R. J. Mason, *Phys. Rev. Lett.* **43**, 1795 (1979).
- <sup>15</sup>N. A. Ebrahim, C. Joshi, D. M. Villeneuve, N. H. Burnett, and M. C. Richardson, *Phys. Rev. Lett.* **43**, 1995 (1979).

## Microinstabilities in the Wendelstein VII A Stellarator Observed by CO<sub>2</sub>-Laser-Light Scattering

J. Meyer

*Department of Physics, The University of British Columbia, Vancouver, British Columbia, V6T1W5, Canada*

and

C. Mahn

*Max-Planck-Institut für Plasmaphysik, EURATOM Association, D-8046 Garching, Germany*

(Received 30 September 1980)

Homodyne detection of scattered CO<sub>2</sub>-laser light demonstrates a close relation between microturbulence level and energy confinement in the Wendelstein VII A stellarator during both Ohmic and neutral-beam heating experiments. With the onset of neutral injection an abrupt order of magnitude decrease in  $(\delta n/n)^2$  accompanied by a broadening of the fluctuation spectra is observed, indicating an almost immediate improvement of containment time.

PACS numbers: 52.35.Py, 52.25.Ps, 52.55.Gb

In present day toroidal plasma confinement experiments anomalous energy transport limits efficient confinement to levels well below that expected from calculations based on classical Coulomb scattering. This anomalous transport can be caused if microinstabilities are driven by the free energy in the confined plasma.<sup>1</sup> The nonlinear nature of the theory makes it extremely difficult to calculate quantitative fluctuation spectra and their influence on energy transport; however, in special cases such influence is strongly suggested.<sup>2</sup> It is therefore desirable to investigate these microturbulences and their effect on energy confinement experimentally.<sup>3-6</sup> In this communication experimental results are discussed which were obtained with CO<sub>2</sub>-laser-light scattering from the Wendelstein VII A (W VII A) stellarator plasma in Garching, Germany, during the period in which a current-free plasma was achieved as discussed in detail in Ref. 5.

The scattered laser radiation is received in

homodyne fashion. 35 W of laser radiation produced by a single-mode cw CO<sub>2</sub> laser is redirected via mirrors over a 10-m path into the W VII A torus into which it is focused by a set of ZnSe lenses to a 3-mm waist. After passing through the torus center the beam is attenuated and reflected from the surface of a BaF<sub>2</sub> plate towards the detector, thus producing 0.1 mW of local oscillator radiation. Scattered radiation after passing through the BaF<sub>2</sub> plate is reflected by a gold-coated surface mirror and is made collinear with the local oscillator beam. The angle and distance between the BaF<sub>2</sub> plate and the gold-coated mirror are chosen such that radiation scattered from 0.5-mm wavelength fluctuations propagating perpendicular to  $B_0$  is detected. Because of the small scattering angle the length of the scattering volume is determined by the plasma diameter. The superimposed beams are then focused onto the HgCdTe detector cooled to 70 °K. Between shots a mirror is placed in the beam path redi-